Dental Research Today

visaga publishing house

Original Research

View Article Online

Received 28 August 2024
Revised 009 September 2024
Accepted 10 September 2024
Available online 16 September 2024

Edited by Mohmed Isaqali Karobari

KEYWORDS:
Protein kinase
PKBα
Virtual Screening
Natural Products
Oral Cancer

Dental Research Today 2024; 1 (1): 26-37
https://doi.org/10.53365/drt/193148
eISSN: XXXX-XXXX

Identification of Potent Inhibitors of Akt Kinases inhibitors from natural sources for Therapeutic Targeting of Oral Squamous Cell Carcinoma

Kannan RR Rengasamy [1,*], Hammad Saleem [2], Balamuralikrishnan Balasubramanian [3]

[1]Centre of Excellence for Pharmaceutical Sciences, North-West University, Potchefstroom, 2520, South Africa
[2]Institute of Pharmaceutical Sciences (IPS), University of Veterinary & Animal Sciences (UVAS), Lahore, Pakistan
[3]Department of Food Science and Biotechnology, College of Life Sciences, Sejong University, Seoul, South Korea

ABSTRACT:

Bagkround: Plant-based natural compounds are effective cancer cell proliferation inhibitors. Consequently, the quest for these compounds for the treatment of cancer has become increasingly competitive and has opened up new avenues for drug development. The current investigation extensively addressed the virtual screening and structure-based prediction of compounds derived from natural products against Protein kinase B-alpha (PKBα, also known as Ak/4GV1).

Materials and Methods: In this study, we conducted a thorough screening of putative PKBα inhibitors from a natural products library, and subsequently performed molecular modeling.

Results: This research identified Irciniastatin B, Irciniastatin A, Pseudoceroxime D, (1'S)-7-chloroaverantin as the top four potential PKBα inhibitors from the library of natural products, whose Glide docking scores range from -10.689 to -7.567 kcal/mol. The RMSD and RMSF analysis reveals that all four ligands remain stable and maintain their interaction throughout the simulation time. The MM/GBSA (ranging from -37.26 to -51.02 kcal/mol) predicted binding affinities are in strong co-relation with that of the docking score, which not only supports the docking results but also suggests that Irciniastatin B exhibits superior binding affinity towards PKBα amongst all four studied compounds. Moreover, the interaction analysis also indicates that Irciniastatin B establishes at least 12 interactions with the neighbouring residues whereas, Irciniastatin A, Pseudoceroxime D, and (1'S)-7-chloroaverantin compounds were able to establish 8-9 interactions in the binding cavity of PKBα. ADMET assessment of the selected compounds was also noted to be within acceptable ranges.

Conclusion: Keeping in view these findings, Irciniastatin B might be a promising candidate for drug discovery against PKBα inhibitors.

1. INTRODUCTION:

Cancer is a prominent cause of mortality worldwide, ranking second in terms of fatality rates and resulting in around 9.6 million deaths during the last several decades, and is responsible for around one in every six deaths worldwide (Feng et al., 2019). According to the World Health Organization (WHO), the number of new cases would rise by nearly 70% over the next two decades, from 14 million to 22 million (Shahzadi et al., 2021), and it was the leading cause of death for 10 million people in 2020 (Sung et al., 2021). At now, cancer treatment options include chemotherapy, surgery, and radiation therapy. Cancer patients have a pressing need and desire for the discovery of innovative compounds that can destroy tumor cells and halt their development without causing severe side effects to the body, as is the case with present

* Corresponding author.
E-mail address: Ragupathi.Rengasamy@nwu.ac.za (Kannan RR Rengasamy)

chemotherapeutic treatments. As a result, the development of novel cancer treatments is a major focus of the researchers and pharmaceutical industry (Roney et al., 2023).

In recent years, research has concentrated on discovering new chemical entities from natural sources in order to meet the immense need for novel kinase inhibitors while also addressing crucial medical diseases, including cancer with connection to signal transduction pathways (Gill et al., 2020). One of these protein kinases is the serine/threonine protein kinase, i.e., protein kinase B (PKB, also known as Akt). It is a target of phosphatidylinositol 3-kinase (PI3K) that plays a crucial function in the PI3K-Akt-mTOR pathway (Barnett et al., 2005). Human PKBs are classified into three subtypes: PKB/Akt-1, PKB/Akt-2, and PKB/Akt-3, which share over eighty percent homology (Fayard et al., 2005; L.H. Wang et al., 2008). The main isoform PKBα is expressed at higher levels (Thakur et al., 2010) and has been a focus for anti-tumor treatment. Activated PKBα can control cell signalling processes by phosphorylating endogenous substrates which are involved in glucose metabolism, cell growth, survival, apoptosis, cell migration, and transcription (Chen et al., 2013). The activity of PKBα is often increased in tumors for many reasons. These include the amplification and functional alterations of receptor tyrosine kinases and PI3K, which are upstream regulators of PKBα. Additionally, the loss of PTEN, a negative regulator of PKBα, can also contribute to its heightened activity in tumors. Anomalous PKBα signaling has been detected in several types of human malignancies, such as breast, prostate, ovarian carcinoma, and melanoma (Fayard et al., 2005). Several PKBα inhibitors have been investigated in clinical trials for the treatment of tumors, including GSK690693 and GDC-0068, which are ATP-competitive inhibitors (Blake et al., 2012), however, the clinical phase I trial of GSK690693 was terminated in 2010 (Chen, Cao et al. 2013). There is still a need to find novel PKBα with an enhanced binding affinity towards PKBα, without causing adverse effects.

Natural products are a valuable and cost-effective resource in the advancement of novel pharmaceuticals, with numerous plant-derived chemicals already being utilized in clinical settings for diverse therapeutic purposes (Ain et al., 2020). The utilization of natural product-derived chemicals and semi-synthetic compounds is a significant avenue for the discovery of novel drug classes (Sinha et al., 2018). In recent years, the field of virtual screening is undergoing tremendous advancements and is serving as a valuable supplement to the high-throughput screening platform in the realm of drug discovery. The presence of these computer platforms facilitates the screening of chemical databases in order to uncover potential matches for the specified targets (Z. Wang et al., 2020). Molecular docking is widely employed as a computational technique in current drug development due to its shown efficacy in accurately predicting ligand binding interactions. Molecular docking is a computational technique that enables the determination of the binding affinity between drugs and protein targets, as well as the elucidation of the underlying mechanism governing this interaction (Sinha et al., 2018). The computational technique is widely regarded as a trustworthy methodology for the large-scale screening of many compounds in order to assess their biological activities and elucidate the mechanisms through which ligands interact with protein targets Waltenberger et al. (2016). The utilization of molecular dynamics (MD) simulations enables a comprehensive examination of the stability and feasibility of binding mechanisms exhibited by the substances. The ADMET characteristics are also computed in order to assess the drug-like qualities of the molecule (Alam et al., 2018). In the present study, we have determined the key structural requirements for protein-ligand interactions of PKBα, for the first time, using an arsenal of computational techniques: ligand (shape)-based virtual screening, molecular docking, molecular electrostatic potential (MESP) analysis, MD simulation, and binding free energy calculation to identify highly potent PKBα inhibitors. Additionally, MD simulation, H-bond occupancy analysis, and binding free energy calculations using implicit MM(GB/PB) SA model were performed for three inhibitors with different potency for PKBα. The results obtained in this study can help to identify potential structural and pharmacophoric features governing the binding process and provide further insights into the key structural modifications for the rational design of novel, potent, and selective PKBα inhibitors.

2. EXPERIMENTAL SECTION

2.1. Target protein and Retrieval of compound structures

The Crystal structure of PKBA alpha in complex with AZD536 (PDB: 4GV1) with a resolution of 1.49 Å (Addie et al., 2013) was retrieved from the protein data bank (PDB) and used for molecular docking studies against the selected compounds from the natural product database. The 3D structures of 1651 compounds were extracted from the Database.

2.2. Preparation of target protein

The three-dimensional structures of the target proteins were prepared using Maestro module 13.7 (Maestro version, 2023-3) in the Schrodinger suite 2023-3. The Crystal structure of PKBA alpha in complex with AZD536 (PDB: 4GV1) with a resolution of 1.49 Å was prepared using the Protein Preparation Wizard in the Maestro module with the force field of OPLS4. The protein preparation process includes deleting water molecules, adding hydrogen atoms, side chains, and missing loops, and removing unwanted metal atoms/ions. The ionization and tautomeric states of the hetero-groups were adjusted. Finally, the optimization steps included optimizing the hydrogen bonds and refining the structure by limiting the RMSD to 0.3 Å. The active binding site residues of PKBA alpha (PDB: 4GV1) were identified using the co-crystal ligand AZD536.

2.3. Ligand preparation

Retrieved compounds were prepared using the LigPrep (Schrodinger Release, 2014) module available in the Schrodinger Suite. All the ligands were minimised with the

force field of OPLS4. A minimum of 32 poses were generated for each ligand. The prepared ligands were further used for molecular docking studies with the target proteins.

2.4. Molecular docking protocol

Molecular docking analysis of the target protein PKBα in complex with AZD536 with compounds (ligands) was performed using the Maestro module in the Schrodinger Suite 2023-3 version. The protein was prepared using Prepwiz, and ligands were prepared using LigPrep in Schrödinger. The grid box was constructed using Receptor Grid generation on the centroid of the protein, and protein-ligand docking was performed using SP (Standard Precision) mode. The top ten percentage of the ligands were further docked using the Extra Precision (XP) mode. The docking output file was analyzed using the Maestro software.

2.5. ADME/Tox

The QikProp module of Maestro Version 13.7 is an absorption, distribution, metabolism, and excretion (ADME) prediction tool that can make certain descriptors of ADME. It makes predictions for both pharmacologically and physico-chemically significant descriptors. Based on Lipinski's rule of five, ADME qualities evaluate the drug-like action of ligand molecules. Maestro Version 13.7 was used to analyze the ADME/T characteristics of the designed compound (Shaikh & Siu, 2016).

2.6. Molecular Mechanics-Generalize Born Surface Area (MM-GBSA)

Molecular docking analysis does not show the relative binding energy or free energy of each ligand or the affinity between the protein and ligand complexes (Pattar et al., 2020). Therefore, MM-GBSA was used to determine the binding energy and free energy between the molecules. It was calculated using Prime MM-GBSA in the Maestro module by uploading the molecular docking output file (. mae format) as the input file.

2.7. Simulation of ligand-receptor interaction

The top-scoring compounds were further evaluated for their stability in ligand-receptor interactions. The top-scoring compounds in the form of protein-ligand complexes were considered. SPC was chosen as the solvent model, and an orthorhombic box was selected. The box size was determined based on the buffer volume, which was minimized before the system was built. The salt concentration of 0.15M with Na^+ and Cl^- was added to the system, and the force field used was OPLS4. The simulation of the prepared ligand-protein complex in the system was run for 100 ns with an energy level of 1.2, and approximately 1000 frames were generated. The ensemble class used was NPT, and the model was relaxed prior to the simulation. The Desmond module available in Maestro v13.7 (Schrodinger v2023-3) was used in this study.

3. RESULTS AND DISCUSSION

3.1. Molecular docking

The co-crystal ligand AZD5363 formed 4 H-bond interactions within the binding pocket. Two of these H-bonds are formed by the pyrazolopyrimidine functionality with GLU228 and ALA230 residues in a donor-acceptor configuration respectively. Both of these amino acids lie within the hinge region, surrounded by a hydrophobic cavity. In addition, this pyrazolopyrimidine moiety of AZD5363 is packed between the hydrophobic chains of the top and bottom amino acid residues, forming π-alky interactions with ALA171, MET227, LEU156, VAL164 (top side), and ALA230, MET281(bottom side). The amine pendant of the co-crystal ligand extends towards the solvent-exposed region mounting two H-bond interactions with GLU234 and GLU278 in close proximity to the catalytic site and the entrance channel. Moreover, para-fluorobenzyl moiety remains settled within a shallow hydrophobic cavity in the N-terminal domain forming a halogen interaction with the electropositive carbonyl carbon and the electronegative para-fluoro substituent. The terminal hyroxyethyl extended within the solvent-exposed region establishing a carbon-Hydogen bond with ASN279.

Table 1
Docking score, Glide score, and Glide emodel results of the top 10 docked structures.

Compound Name	Docking Score	Glide Score	Glide emodel
Irciniastatin B	-10.689	-10.701	-110.53
Irciniastatin A	-8.145	-8.157	-106.832
Pseudoceroxime D	-7.809	-8.575	-100.084
$C_{20}H_{19}ClO_7$	-7.567	-8.736	-77.166
Streptonaphthyridine A	-7.408	-7.408	-40.592
Acremochlorin G	-7.132	-7.166	-79.584
11S-(−)-penilloid A	-6.882	-6.987	-71.259
11R,14E-(+)-penilloid A	-6.821	-6.926	-67.209
Pseudoceroxime B	-6.692	-6.887	-107.669
Hyrtioerectine F	-6.535	-6.669	-71.774

Based on the lowest docking score the top ten docked ligands are tabulated in Table 1. The chemical structures of top scoring compounds were given in Figure 1. The docking scores are also augmented by the glide score and glide e-model results. Among these selected compounds the top 4 compounds (Irciniastatin B, Irciniastatin A, Pseudoceroxime D, (1'S)-7-chloroaverantin) were subjected to MD-simulation studies in order to validate the findings of the dicking experiment. The ligand Hydrogen bond (H-bond) interactions, MMGBA of the aforementioned four compounds are detailed in the Tables 2 and 3. The compound Irciniastatin B showed better binding within the 4GV1 binding pocket with 7 H-bond interactions compared to the 6 H-bonds formed by the AZD5363 within the same binding site. The lead compound Pseudoceroxime D, with 6 H-bonds showed comparable docking profiles with the AZD5363, co-crystal

Table 2
Ligand interactions of top four compounds.

Compound Name	Docking score(kcal/mol)	Glide gscore(kcal/mol)	Glide emodel	Interacting Residues with H-bond	Bond Length (Å)
Irciniastatin B	-10.689	-10.701	-110.530	A230;E228; K179; D292; F161; K276; D274	2.41, 1.95, 2.01, 2.37, 2.38, 1.82, 1.67
Irciniastatin A	-8.145	-8.157	-106.832	E228; K179; K276; D274	2.49; 2.32; 2.17; 1.89
Pseudoceroxime D	-7.809	-8.575	-100.084	K179; K276; D292; E228 A230	2.15; 2.23; 2.40; 2.53; 2.11; 1.65
(1'S)-7-chloroaverantin	-7.567	-8.736	-77.166	E228; D292; E234	2.72; 1.53; 1.75

ligand.

All docked structures occupy the same binding cavity with a few differences in binding interactions. The H-bond interactions in the hinge regions seems imperative for the ligand binding and interestingly enough the H-bond interaction with ALA230 is retained by Irciniastatin B and Pseudoceroxime D, while (1'S)-7-chloroaverantin retains the H-bond interaction with GLU234 in the solvent-exposed region. It is important to note that the lead compounds provided a different binding profile in comparison with the co-crystal ligands as all the H-bonds were formed with residues within the binding pocket. In terms of docking similarity, the ALA230 bond was common with the nascent ligand in 2 lead molecules (Irciniastatin B and Pseudoceroxime D) and the parent interaction of GLU234 was conserved in the docking of (1'S)-7-chloroaverantin, which was also the structure with the minimum number of H-bonds (3 in total). A new H-bond was formed with the GLU228 residue by all the lead compounds and the top three leads also formed an H-bond with LYS179 residue.

This drastic difference in binding profiles from the parent AZD5363 ligand and the lack of commonality between the individual leads too for that matter can be attributed to their widely different chemical structures. Only the isomeric leads Irciniastatin B and Irciniastatin A depicted identical binding profiles with the former having two additional H-bonds than the latter. The shape similarity of a molecule with an existing active molecule or a drug, does not necessarily imply that the new molecule should also possess similar activity potential. However, the shape along with appropriate chemical functionality are key factors for a compound to possess activity against a specific target. Thus, a combination of structural similarity mated with the chemical/steric functionality may allow structurally diverse molecules to exhibit similar biological potential i.e. structurally dissimilar moieties may adopt similar active profiles within the same binding pocket dictated by the steric and chemical interactions mounted within the same binding pocket. This may explain comparable results obtained during both molecular docking and MD simulation experiments as the volume overlap of two molecules is analogous despite the structural diversity.

Table 3
MM-GBSA results of the top four compounds

Compound Name	Docking score (kcal/mol)	MM-GBSA Binding Energy (kcal/mol)
Irciniastatin B	-10.689	-51.02
Irciniastatin A	-8.145	-37.48
Pseudoceroxime D	-7.809	-37.26
(1'S)-7-chloroaverantin	-7.567	-51.42

3.2. ADMET

The use of computational ADMET screening has the potential to decrease the expenses associated with resource-intensive wet-lab studies, which often result in failure on several occasions (Hage-Melim et al., 2020; Zhang et al., 2020). In the present investigation, it was observed that all of the molecules that were chosen adhered to the optimal threshold of ADMET characteristics. The compounds exhibit alignment within the permissible range of -2.0 to 6.5 for the octanal/water partition coefficient (QPlogPo/w), -6.5 to 0.5 for the aqueous solubility (QPlogS), and -3.0 to 2.1 for the brain/blood partition coefficient (QPlogBB) (Table 4) (Gleeson et al., 2009). The evaluation of drug candidates for their compliance with established criteria of drug-likeness and physiochemical properties is a crucial preliminary screening procedure, with the objective of identifying and eliminating unsuitable candidates (Mohamed et al., 2021). The Lipinski's rule of five (RO5) is a significant determinant in assessing the drug-likeness of compounds. It assists in the identification of potential molecules from a collection of drug-like substances that should possess favorable characteristics such as robust gastrointestinal absorption, high oral bioavailability, and adequate membrane permeability. These desirable properties are indicated by the following criteria: a logarithm of the partition coefficient (log P) less than or equal to 5, a molecular weight (MW) less than or equal to 500 Da, a number of hydrogen bond donors (HBDs) less than or equal to 5, and a number of hydrogen bond acceptors (HBAs) less than or equal to 10 (Manivannan et al., 2022), and these parameters for the studied compounds were noted to be within the acceptable ranges (Table 4).

Table 4
ADME/Tox properties of the top four selected compounds that exhibited a high binding efficiency.

Title (and Range)	Irciniastatin B	Irciniastatin A	Pseudoceroxime D	(1'S)-7-chloroaverantin
#amine (0–1)	0	0	0	0
#amidine (0)	0	0	0	0
#acid (0–1)	0	0	0	0
#amide (0–1)	1	1	0	0
rotor	16	17	14	10
#rtvFG	1	1	1	0
CNS (-2 inactive and +2 active)	-2	-2	-2	-2
mol MW (130.0–725.0)	607.697	609.712	775.039	406.819
Dipole (1.0–12.5)	0	0	0	0
SASA (300.0–1,000.0)	866.983	912.344	825.691	644.126
FOSA (0.0–750.0)	549.185	564.09	241.877	218.573
FISA (7.0–330.0)	233.615	254.138	246.467	254.7
PISA (0.0–450.0)	84.183	94.116	87.86	109.041
WPSA (0.0–175.0)	0	0	249.487	61.813
Volume (500.0–2000.0)	1755.203	1802.151	1532.228	1150.076
donorHB (0.0–6.0)	4	5	4	3
accptHB (2.0–20.0)	16.5	16.2	11.65	6.7
dip^2/V (0.0–0.13)	0	0	0	0
ACxDN^.5/SA (0.0–0.05)	0.038063	0.039705	0.028219	0.018016
Glob (0.75–0.95)	0.811657	0.784996	0.778448	0.82416
QPpolrz (13.0–70.0)	54.62	55.951	47.015	34.492
QPlogPC16 (4.0–18.0)	17.455	18.514	17.615	12.577
QPlogPoct	33.861	35.242	29.451	21.075
QPlogPw	23.744	24.483	18.313	12.552
QPlogPo/w (-2.0–6.5)	1.056	1.15	3.019	2.036
QPlogS (-6.5–0.5)	-3.066	-3.918	-5.787	-4.153
CIQPlogS	-4.763	-4.799	-10.93	-5.52
QPlogHERG	-3.607	-4.085	-5.536	-4.897
QPPCaco (<25 poor, >500 great)	44.872	32.653	45.567	38.069
QPlogBB (-3.0–1.2)	-2.765	-3.211	-2.38	-2.387
QPPMDCK (<25 poor, >500 great)	23.782	14.652	408.51	31.531
QPlogKp (-8.0 to −1.0)	-3.992	-4.24	-4.408	-4.869
IP (eV) (7.9–10.5)	0	0	0	0
EA (eV) (-0.9–1.7)	0	0	0	0
#metab	12	12	5	5
QPlogKhsa (-1.5–1.5)	-0.79	-0.729	-0.16	-0.033
Human Oral Absorption	1	1	2	3
Percent Human Oral Absorption (>80% is high, <25% is poor)	36.776	21.902	48.391	67.153
SAfluorine	0	0	0	0
SAamideO	16.15	9.045	0	0
PSA	182.467	173.992	177.575	147.226
#NandO	12	12	11	7
Rule Of Five (maximum is 4)	2	3	2	0
#ringatoms	16	16	17	14
#in34	0	0	0	0
#in56	16	16	17	14
#noncon	6	7	2	0
#nonHatm	43	43	37	28
Jm	0.053	0.004	0	0
Rule Of Three (maximum is 3)	1	1	1	0

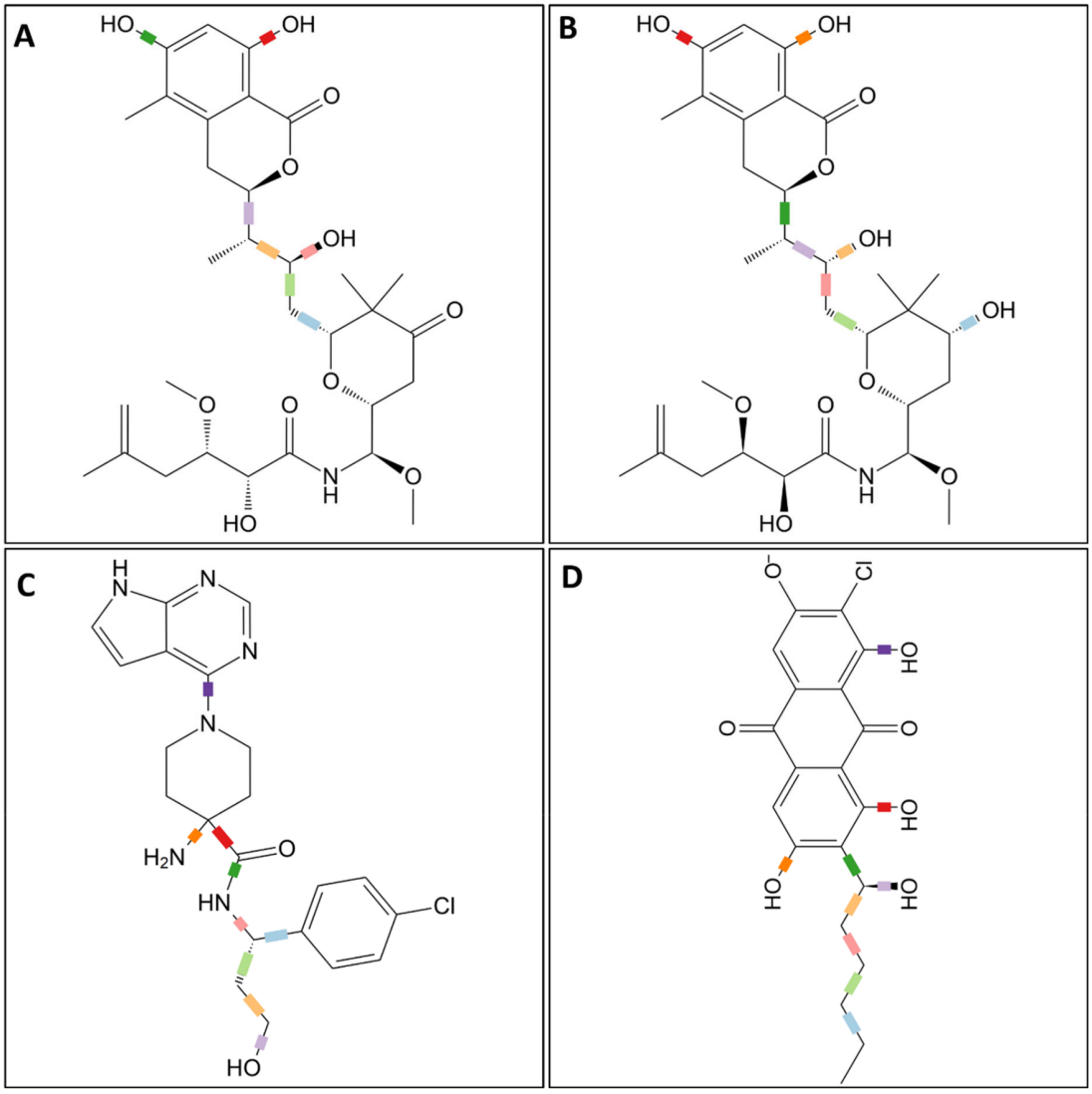

Figure 1. 2D chemical structures of Top four compounds.

3.3. Dynamic Simulations, Comprehensive Analysis of Structural Flexibility and Stability of top scoring compounds

Top four docking complexes Irciniastatin B-PKBα, Irciniastatin A-PKBα, Pseudoceroxime D-PKBα and (1'S)-7-chloroaverantin- PKBα were post- processed with MD simulations the stability of the studied complexes was elucidated by computing RMSD during simulation. All complexes stable during the simulation period and RMSD remained below 2.5 Å for protein or ligand (Figure 3). Among all four complexes, the least RMSD was found to be displayed by Irciniastatin B in Irciniastatin B-PKBα bonded system (Figure 3A); which confirms that the compound Irciniastatin B is firmly bonded to PKBα. The RMSD curve for protein fluctuated between 1.2 to 2.4 Å, which reflects the conformational changes in protein structure without disrupting the structure. Interestingly, compound Irciniastatin B shows a high level of stability throughout the time duration 100ns, which strongly suggests that the Irciniastatin B maintained its initial conformation throughout the simulation and did not lose any major interaction. The same results are confirmed by the highest value of docking scores. In the case of CP1575/1 bonded system, compound CP1575/1 showed a minor fluctuation during the initial frames of the MD simulation. However, the fluctuation is not too high and the Irciniastatin A-PKBα system acquired equilibrium after 20ns. As shown in Figure 3B, both ligand and protein in the Irciniastatin A-PKBα complex remained stable after 40ns of MD simulation. Among all four complexes (Figure 3) (1'S)-7-chloroaverantin-PKBα complex (Figure 3D) showed the highest fluctuations with the biggest RMSD values of ~2.1 Å and ~2.3 Å for protein and ligand, respectively, indicating that (1'S)-7-chloroaverantin is weakly bonded to PKBα (Figure 4B). Pseudoceroxime D has also shown some fluctuation in Pseudoceroxime D- PKBα complex. As shown in Figure 3C, Pseudoceroxime D remained highly stable during initial snapshots (1-65ns), however, a jump

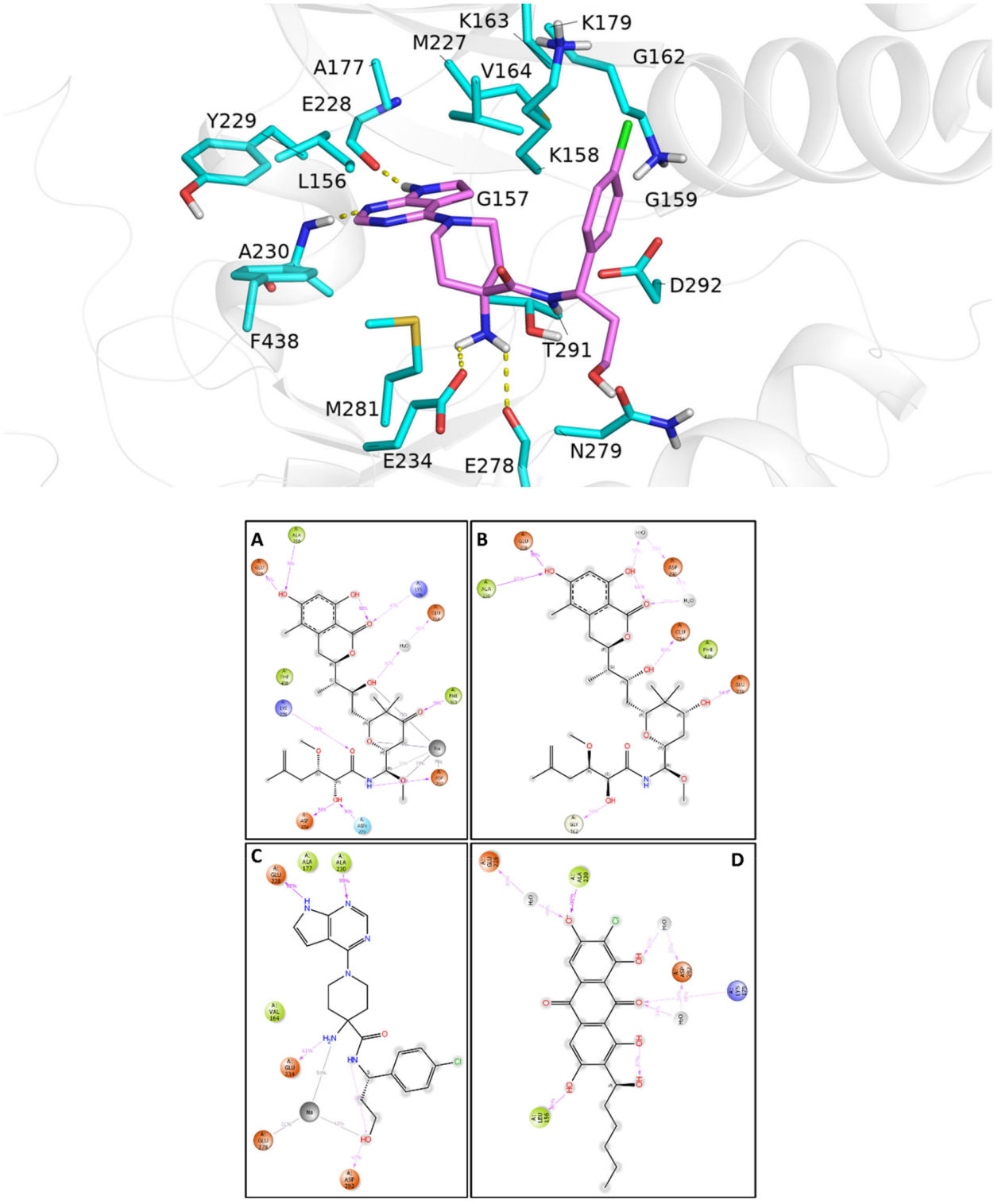

Figure 2. Aminoacid interactions of the selected rine compounds in the identified active site.

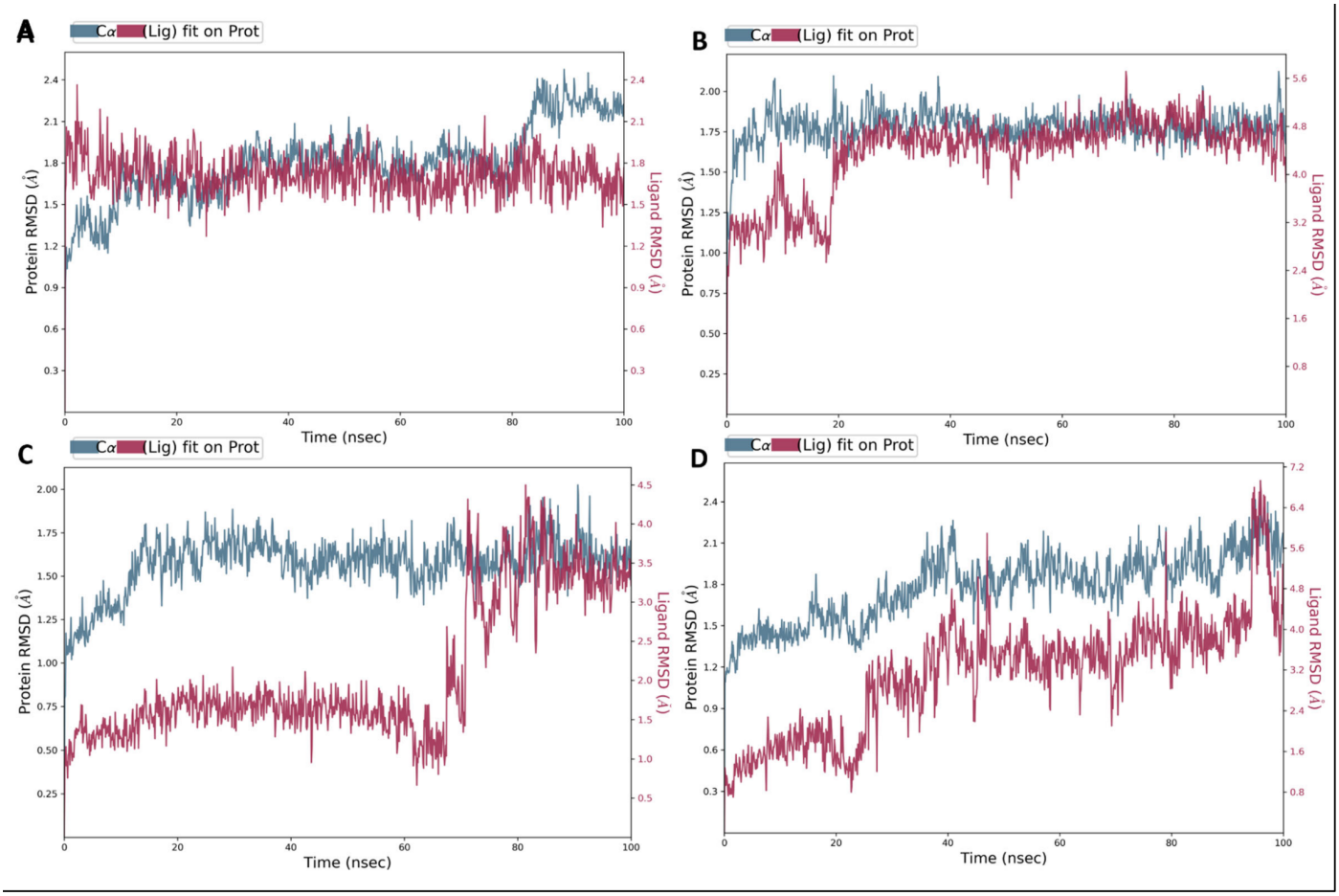

Figure 3. RMSD plots of the protein portion (blue) and Compoundsrelated to the MD simulations.

of ∼1.1 Å in the RMSD curve was obtained at 67ns and the system immediately acquired equilibrium. Again, these facts are also in accordance with the docking results, which suggest that the compounds Irciniastatin B and Irciniastatin A are more firmly bonded to PKBα than that of Pseudoceroxime D and (1'S)-7-chloroaverantin. Figure 4A-D depicts the RMSF versus the residue number and the RMSF of the PKBα's residues from the MD trajectory appears same trend which obtained from from the X-ray crystallographic data. This result suggests that the Irciniastatin B exhibited higher conformational changes in the structure of PKBα with M281L.

Molecular docking analysis does not show the relative binding energy or free energy of each ligand or the affinity between the protein and ligand complexes (Pattar et al., 2020). Therefore, an exhaustive analysis of the computed binding affinities of Irciniastatin B, Irciniastatin A, Pseudoceroxime D, and (1'S)-7-chloroaverantin towards PKBα has been performed by employing the MM/PB(GB)SA approach. The obtained binding affinities of ligand-protein complexes were then summarized in Table 2 to compare with the binding affinities of selected molecules bonded to PKBα. The binding free energy values $\Delta G_{pred(GB)}$ computed byMM/PB(GB)SAapproachreveals that the compounds Irciniastatin B with the highest docking scores also exhibit the highest binding affinity (-29.85 kcal·mol^{-1}) towards PKBα and are more strongly bonded to the studied protein than that of Irciniastatin A, Pseudoceroxime D and (1'S)-7-chloroaverantin. Since Irciniastatin B showed the most significant difference in ΔG_{pred} values for PKBα in contrast to other compounds; it reflects that the compound Irciniastatin B is the most potent PKBα inhibitor among all four inhibitors. Similarly, in the PKBα -bonded system, Irciniastatin A, and Pseudoceroxime D demonstrate comparable binding affinities to each other (ΔG_{pre} –37.48 and -37.26 kcal•mol^{-1}, respectively) for PKBα. Last but not the least, compound (1'S)-7-chloroaverantin has also demonstrated appreciable affinity towards PKBα (ΔG_{pre} –37.48 kcal•mol^{-1}). Taking together, MMGBSA results are in strong correlation with the findings of docking analysis and suggest that the Irciniastatin B could be the most potent PKBα inhibitor among all four selected compounds. Although, compound(1'S)-7-chloroaverantin shares the least binding affinity in terms of docking scores, high MMGBSA binding affinity presents (1'S)-7-chloroaverantin as a potential PKBα inhibitor.

To pinpoint the essential amino acids that effectively maintained contact with ligands within the PKBα complex, we

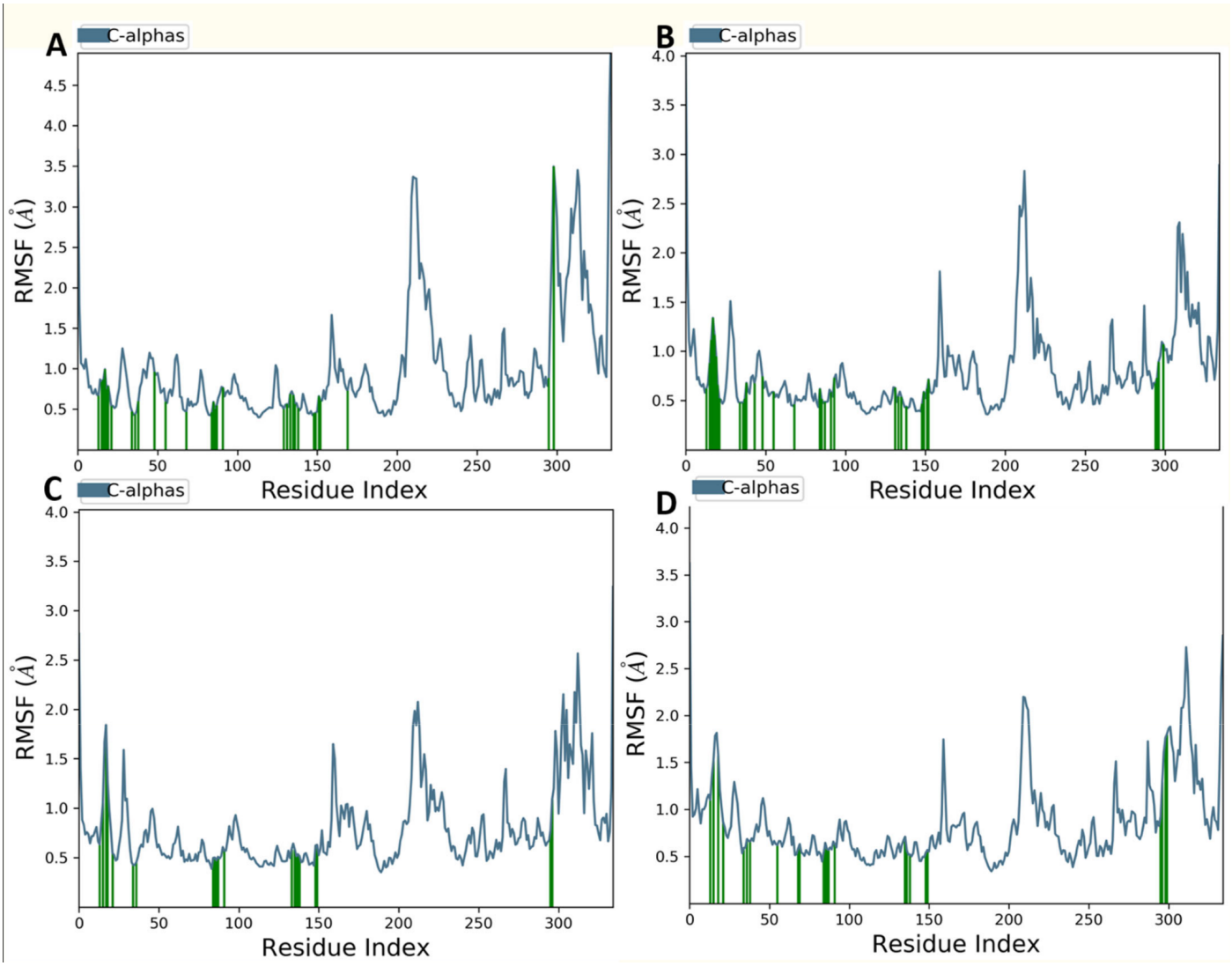

Figure 4. RMSF plots of the protein portion (blue) and Compounds related to the MDsimulations.

generated a timeline representation illustrating various interactions such as hydrogen bonds, hydrophobic interactions, ionic interactions, and water bridges, as shown in Figure 5. Notably, during both docking and MMGBSA analysis, Irciniastatin B exhibited the highest binding affinity for PKBα. These findings were further substantiated by the protein-ligand contact analysis chart, as illustrated in Figure 4A, where Irciniastatin B consistently established and sustained approximately twelve interactions with adjacent residues. Within the Irciniastatin B-PKBα complex system, amino acids T160, M227, A230, Y272, D274, K276, E278, N279, and D292 emerge as the pivotal residues, consistently maintaining contact with the ligand for more than 80% of the observed duration. The top panel shows the total number of specific contacts the protein makes with the ligand over the course of the trajectory. Conversely, Irciniastatin A, Pseudoceroxime D, and (1'S)-7-chloroaverantin in their corresponding complexes were able to establish and maintain at least eight contacts with the closely available residues (Figure 5B-D). It's intriguing to observe that certain amino acid residues, namely E228, A230, E234, E278, and D292, exhibit a consistent interaction pattern across all studied ligands Irciniastatin B, Irciniastatin A, Pseudoceroxime D, and (1'S)-7-chloroaverantin when bound to PKBA. These residues seem to play a key role in forming stable contacts with the ligands. Moreover, the residue D292, which is conserved across these systems, stands out as it forms more than one specific interaction with the ligands in all of the analyzed cases. This enhanced level of interaction is represented graphically by a darker shade of orange on the colour scale located to the right of the plot, highlighting the significance of this particular residue in the binding process. In summary, the results from our current analysis align well with the docking outcomes, confirming that all four chosen ligands exhibit significant binding affinities for PKBα. Notably, Irciniastatin B stands out as it demonstrates superior binding affinity compared to the other ligands studied, primarily due to its ability to establish additional interactions

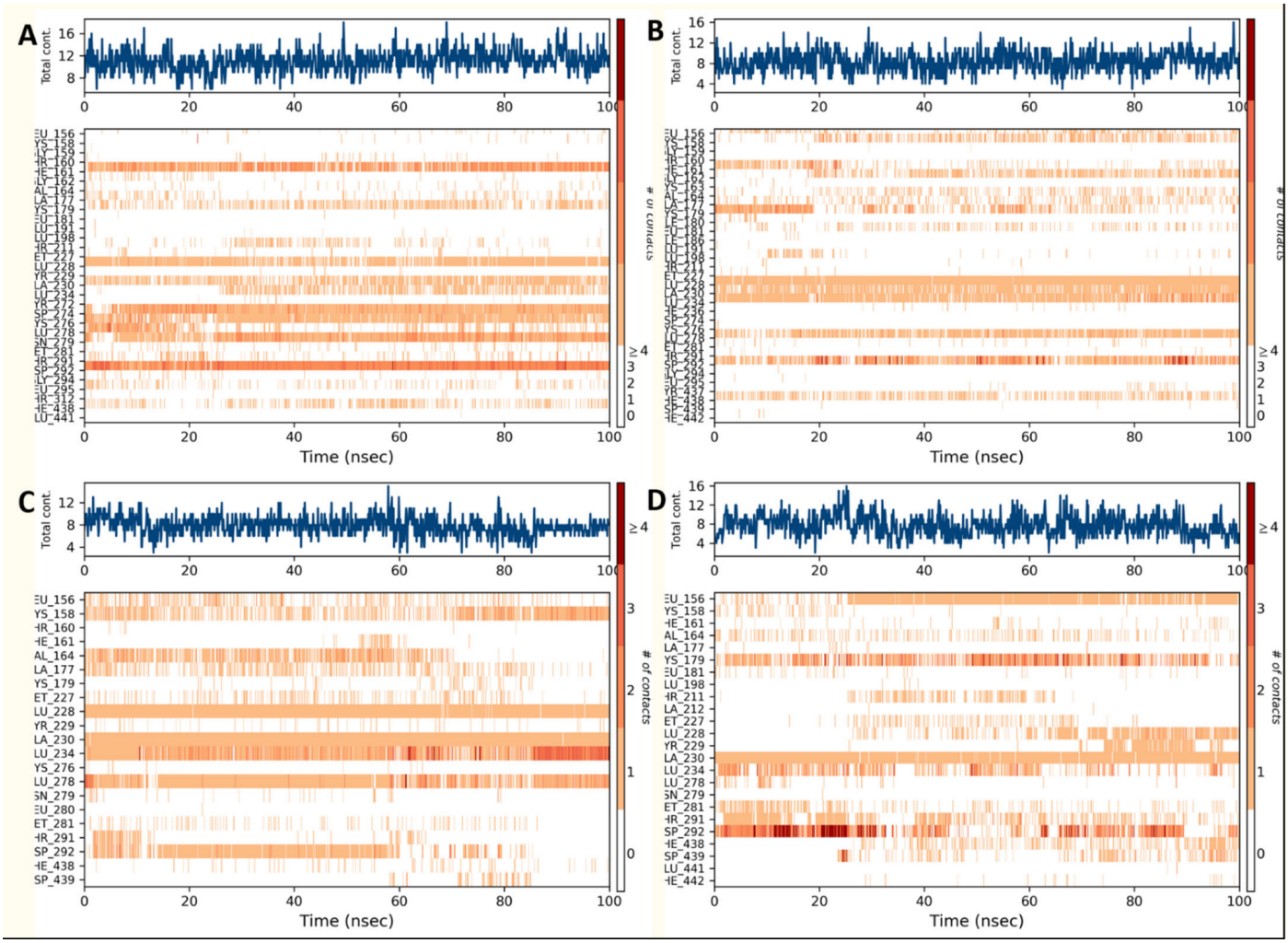

Figure 5. SSE interactions Timeline related to the MD simulations.

with neighbouring residues.

4. CONCLUSION

This study undertook a comprehensive investigation of natural substances as possible inhibitors of Protein Kinase B-alpha (PKBα), a critical target in the field of cancer treatment. By employing virtual screening and employing structure-based predictions, we have identified Irciniastatin B as a very promising candidate for therapeutic development. This compound has exceptional binding affinity and establishes a strong network of interactions with PKBα. The results of our study are substantiated by employing a comprehensive approach that includes molecular docking, MM/GBSA binding energy calculations, molecular dynamics simulations, and ADMET evaluations. The confirmation of the stability of PKBα-ligand complexes was achieved by conducting thorough molecular dynamics simulations, which emphasized the persistent connections between the ligands and crucial residues of the protein. Moreover, there is a good correlation between the anticipated binding affinities and the docking scores, which serves to enhance the credibility and dependability of our findings. In conclusion, our study showcases the potential of naturally occurring chemicals, specifically Irciniastatin B, as very promising contenders for the advancement of PKBα inhibitors in the realm of cancer therapy. The aforementioned discoveries not only contribute to the advancement of our comprehension of the molecular interactions implicated, but also present novel opportunities for the exploration of therapeutic agents in the ongoing battle against cancer. The ongoing exploration of plant-derived natural chemicals as inhibitors of cancer cell proliferation is a highly competitive and productive field of research, holding promise for the development of more efficacious cancer treatments in the coming years.

5. DATA AVAILABILITY STATEMENT

The data presented in this study are available on request from the corresponding authors.

CONFLICTS OF INTEREST

There is no conflict of interest.

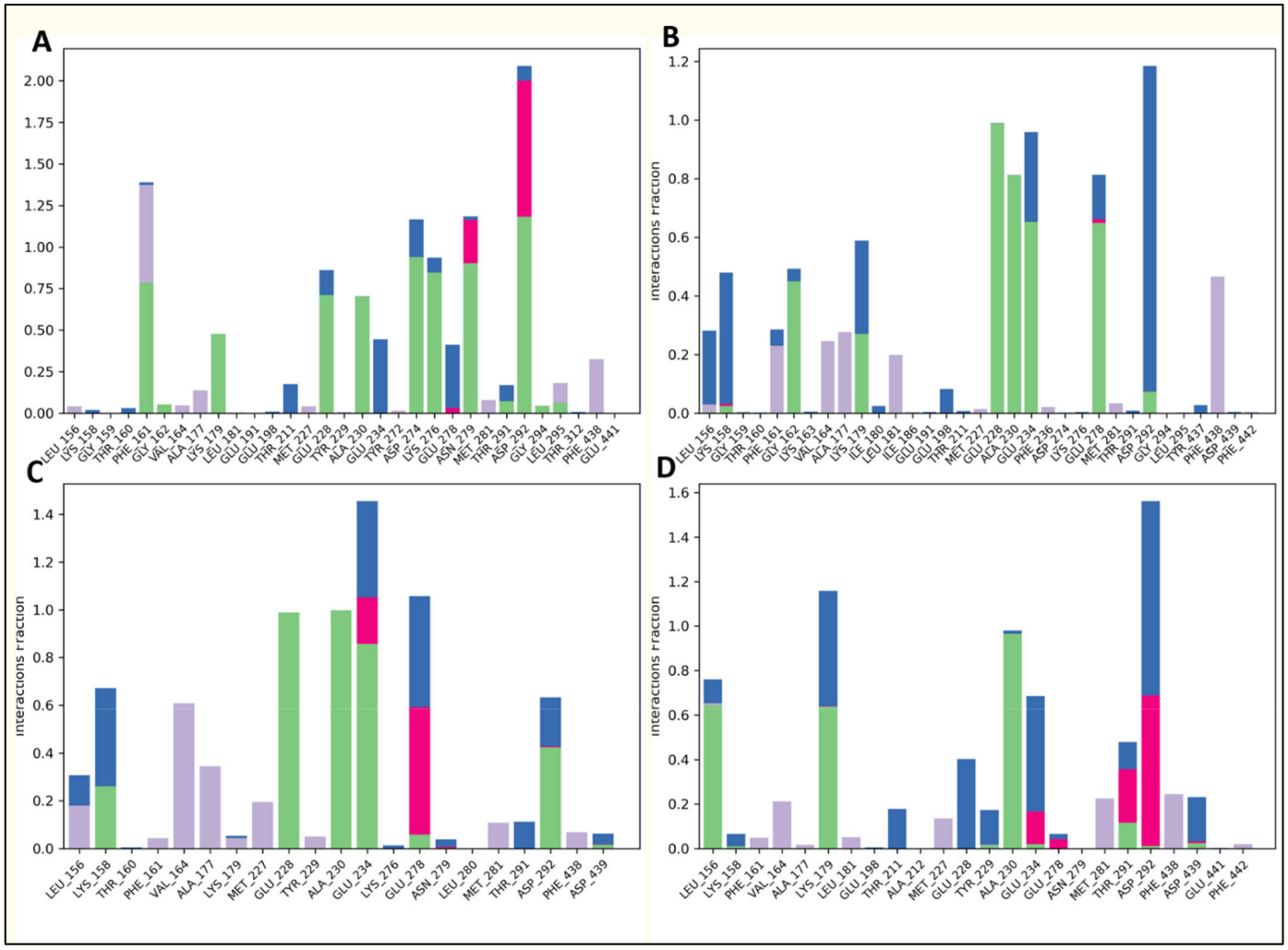

Figure 6. Protein–ligand interactions histogram related to theMD simulation.

ACKNOWLEDGMENTS

Kannan RR Rengasamy acknowledges the Centre for High Performance Computing (CHPC), South Africa, for providing computational resources to this research project.

ORCID

Kannan RR Rengasamy 0000-0001-7205-7389
Hammad Saleem 0000-0002-2541-0271
Balamuralikrishnan Balasubramanian 0000-0001-6938-1495

AUTHOR CONTRIBUTIONS

Conceptualization, K.R.R.R; writing-original manuscript, KRRR, HS; Methodology, data curation, and formal analysis, KRRR, BB; Project administration and Supervision, K.R.R.R; Review and editing, KRRR, BB, HS.; Interpretation, and review/revision, B.B and K.R.R.R. All authors have read and agreed to the published version of the manuscript.

REFERENCES

Addie, M., Ballard, P., Buttar, D., Crafter, C., Currie, G., Davies, B.R., Debreczeni, J., Dry, H., Dudley, P., Greenwood, R., 2013. Discovery of 4-Amino-N-[(1 S)-1-(4-chlorophenyl)-3-hydroxypropyl]-1-(7 H-pyrrolo [2, 3-d] pyrimidin-4-yl) piperidine-4-carboxamide (AZD5363), an Orally Bioavailable, Potent Inhibitor of Akt Kinases. Journal of Medicinal Chemistry. 56(7), 2059–2073. https://doi.org/10.1021/jm301762v

Ain, Q.U., Batool, M., Choi, S., 2020. TLR4-targeting therapeutics: structural basis and computer-aided drug discovery approaches. Molecules. 25(3), 627. https://doi.org/10.3390/molecules25030627

Alam, M., Alam, M.J., Azaz, S., Parveen, M., Park, S., Ahmad, S., 2018. DFT/TD-DFT calculations, spectroscopic characterizations (FTIR, NMR, UV-vis), molecular docking and enzyme inhibition study of 7-benzoyloxycoumarin. Computational Biology and Chemistry. 73, 65–78. https://doi.org/10.1016/j.compbiolchem.2018.01.007

Barnett, S.F., Bilodeau, M.T., Lindsley, C.W., 2005. The Akt/PKB family of protein kinases: a review of small molecule inhibitors and progress towards target validation. Current Topics in Medicinal Chemistry. 5(2), 109–125. https://doi.org/10.2174/1568026053507714

Blake, J.F., Xu, R., Bencsik, J.R., Xiao, D., Kallan, N.C., Schlachter, S., Mitchell, I.S., Spencer, K.L., Banka, A.L., Wallace, E.M., 2012. Discovery and preclinical pharmacology of a selective ATP-competitive

Akt inhibitor (GDC-0068) for the treatment of human tumors. Journal of Medicinal Chemistry. 55(18), 8110–8127. https://doi.org/10.1021/jm301024w

Chen, S.F., Cao, Y., Chen, J.J., Chen, J.Z., 2013. Binding selectivity studies of PKBα using molecular dynamics simulation and free energy calculations. Journal of Molecular Modeling. 19, 5097–5112. https://doi.org/10.1007/s00894-013-1997-3

Fayard, E., Tintignac, L.A., Baudry, A., Hemmings, B.A., 2005. Protein kinase B/Akt at a glance. Journal of Cell Science. 118(24), 5675–5678. https://doi.org/10.1242/jcs.02724

Feng, R.M., Zong, Y.N., Cao, S.M., Xu, R.H., 2019. Current cancer situation in China: good or bad news from the 2018 Global Cancer Statistics? Cancer Communications. 39(1), 1–12. https://doi.org/10.1186/s40880-019-0368-6

Gill, M.S., Saleem, H., Ahemad, N., 2020. Plant extracts and their secondary metabolites as modulators of kinases. Current topics in medicinal chemistry. 20(12), 1093–1104.

Gleeson, P., Bravi, G., Modi, S., Lowe, D., 2009. ADMET rules of thumb II: a comparison of the effects of common substituents on a range of ADMET parameters. Bioorganic & Medicinal Chemistry. 17(16), 5906–5919. https://doi.org/10.1016/j.bmc.2009.07.002

Hage-Melim, L.I.D.S., Federico, L.B., De Oliveira, N.K.S., Francisco, V.C.C., Correia, L.C., De Lima, H.B., Gomes, S.Q., Barcelos, M.P., Francischini, I.A.G., 2020. Virtual screening, ADME/Tox predictions and the drug repurposing concept for future use of old drugs against the COVID-19. Life Sciences. 256, 117963. https://doi.org/10.1016/j.lfs.2020.117963

Manivannan, A.C., Malaisamy, A., Eswaran, M., Meyyazhagan, A., Arumugam, V.A., Rengasamy, K.R., Balasubramanian, B., Liu, W.C., 2022. Evaluation of clove phytochemicals as potential antiviral drug candidates targeting SARS-CoV-2 main protease: Computational Docking, molecular dynamics simulation, and pharmacokinetic profiling. Frontiers in Molecular Biosciences. 9, 918101. https://doi.org/10.3389/fmolb.2022.918101

Mohamed, H.S., El-Serwy, W.S., El-Serwy, W.S., 2021. Synthesis, molecular docking, In silico ADME predictions, and toxicity studies of N-substituted-5-(4-chloroquinolin-2-yl)-1, 3, 4-thiadiazol-2-amine derivatives as COVID-19 inhibitors. Russian Journal of Bioorganic Chemistry. 47, 158–165. https://doi.org/10.1134/S1068162021010155

Pattar, S.V., Adhoni, S.A., Kamanavalli, C.M., Kumbar, S.S., 2020. In silico molecular docking studies and MM/GBSA analysis of coumarin-carbonodithioate hybrid derivatives divulge the anticancer potential against breast cancer. Beni-Suef University Journal of Basic and Applied Sciences. 9(1), 1–10. https://doi.org/10.1186/s43088-020-00059-7

Roney, M., Dubey, A., Nasir, M.H., Tufail, A., Tajuddin, S.N., Aluwi, M.F.F.M., Huq, A.M., 2023. Computer-aided anti-cancer drug discovery of EGFR protein based on virtual screening of drug bank, ADMET, docking, DFT and molecular dynamic simulation studies. Journal of Biomolecular Structure and Dynamics, 1–16. https://doi.org/10.1080/07391102.2023.2252092

Shahzadi, I., Zahoor, A.F., Rasul, A., Mansha, A., Ahmad, S., Raza, Z., 2021. Synthesis, Hemolytic Studies, and In Silico Modeling of Novel Acefylline-1, 2, 4-Triazole Hybrids as Potential Anti-cancer Agents against MCF-7 and A549. ACS Omega. 6(18), 11943–11953. https://doi.org/10.1021/acsomega.1c00424

Shaikh, F., Siu, S.W., 2016. Identification of novel natural compound inhibitors for human complement component 5a receptor by homology modeling and virtual screening. Medicinal Chemistry Research. 25, 1564–1573. https://doi.org/10.1007/s00044-016-1591-1

Sinha, S., Doble, M., Manju, S., 2018. Design, synthesis and identification of novel substituted 2-amino thiazole analogues as potential anti-inflammatory agents targeting 5-lipoxygenase. European Journal of Medicinal Chemistry. 158, 34–50. https://doi.org/10.1016/j.ejmech.2018.08.098

Sung, H., Ferlay, J., Siegel, R.L., Laversanne, M., Soerjomataram, I., Jemal, A., Bray, F., 2021. Global cancer statistics 2020: GLOBOCAN estimates of incidence and mortality worldwide for 36 cancers in 185 countries. CA: A Cancer Journal for Clinicians. 71(3), 209–249. https://doi.org/10.3322/caac.21660

Thakur, D.S., Kumar, P., Kumar, P., C., 2010. Akt: a new approach for cancer treatment. International Journal of Pharmaceutical Sciences and Research. 1(suppl8), 29–36.

Waltenberger, B., Atanasov, A.G., Heiss, E.H., Bernhard, D., Rollinger, J.M., Breuss, J.M., Schuster, D., Bauer, R., Kopp, B., Franz, C., 2016. Drugs from nature targeting inflammation (DNTI): a successful Austrian interdisciplinary network project. Monatshefte für Chemie-Chemical Monthly. 147, 479–491. https://doi.org/10.1007/s00706-015-1653-y

Wang, L.H., Cheng, G.Z., Park, S., Shu, S., He, L., Kong, W., Zhang, W., Yuan, Z., Cheng, J.Q., 2008. Advances of AKT pathway in human oncogenesis and as a target for anti-cancer drug discovery. Current Cancer Drug Targets. 8(1), 2–6. https://doi.org/10.2174/156800908783497159

Wang, Z., Sun, H., Shen, C., Hu, X., Gao, J., Li, D., Cao, D., Hou, T., 2020. Combined strategies in structure-based virtual screening. Physical Chemistry Chemical Physics. 22(6), 3149–3159. https://doi.org/10.1039/C9CP06303J

Zhang, T., Cui, X., Zhao, X., Wang, J., Zheng, J., Zheng, G., Guo, W., Cai, C., He, S., Xu, Y., 2020. Detectable SARS-CoV-2 viral RNA in feces of three children during recovery period of COVID-19 pneumonia. Journal of Medical Virology. 92(7), 909–914. https://doi.org/10.1002/jmv.25795